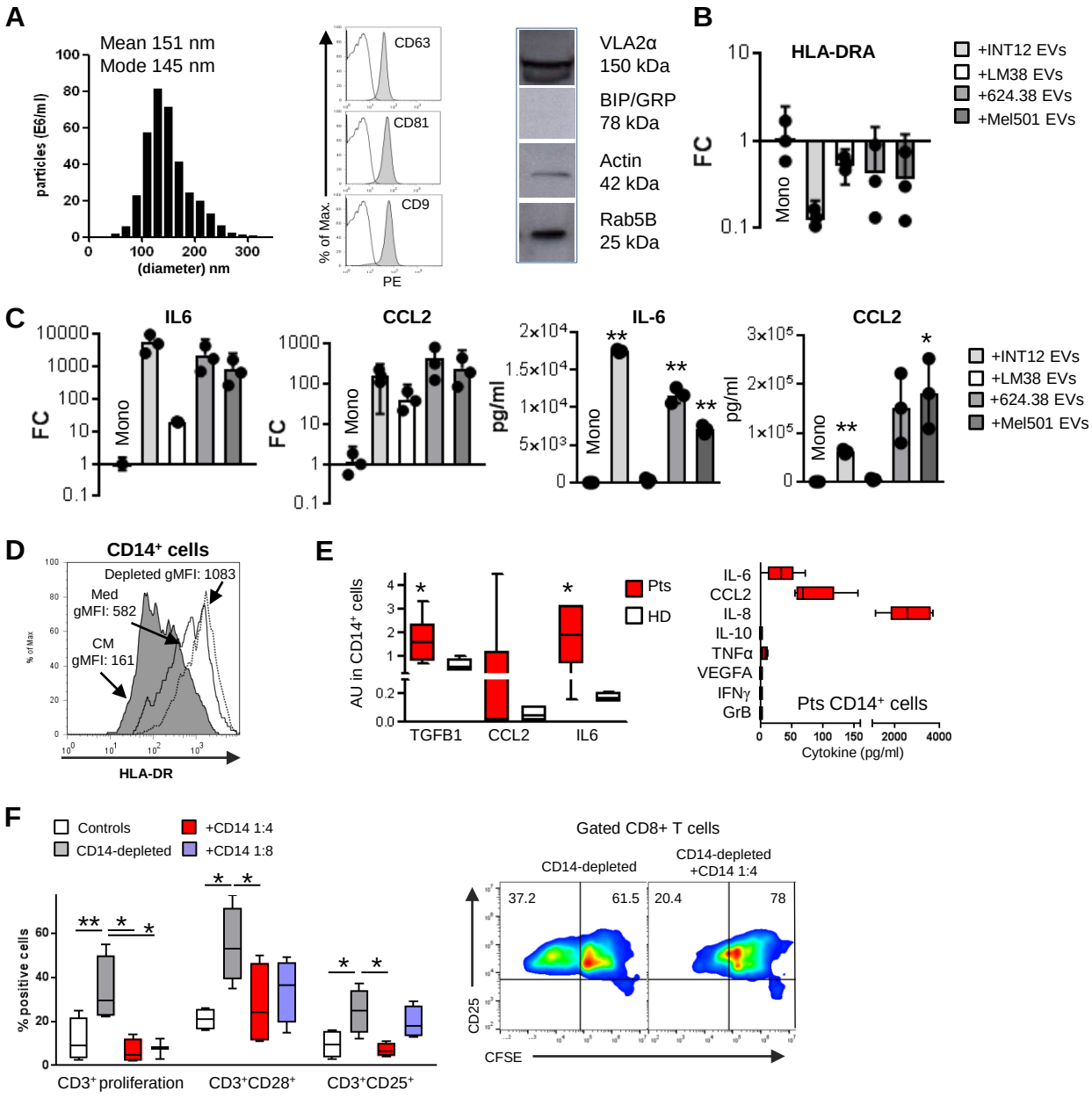

Supplemental Figure 1. Melanoma EVs convert myeloid cells into MDSCs. (**A**) Particle concentration and distribution by NTA in a preparation of melanoma EVs isolated from conditioned medium of INT12 melanoma cells (left). Expression of EV markers CD63, CD81 and CD9 determined by flow cytometry after incubation with specific PE-conjugated Abs of latex bead-coupled EVs (middle). Western blot analysis of EV marker Rab5B, actin and VLA2α. The absence of BIP protein confirmed purity of isolated vesicles (right). Data shown are representative of 5 melanoma EV preparations. (**B, C**) HLA-DRA, IL6 and CCL2 expression and production in monocytes conditioned or not with melanoma EVs from different cell lines (INT12, LM38, 624.38 and Mel501). (**D**) HLA-DR expression, measured by flow cytometry in HD monocytes after incubation with EV depleted (Depleted) compared to undepleted conditioned medium (CM) and to control medium (Med). (**E**) Cytokine expression in isolated CD14⁺ cells from patients and HD (n=6/group) (left), and cytokine production (right). (**F**) T cell proliferation of PBMCs from melanoma patients (n=4) after mock depletion, depletion of CD14⁺ cells and re-addition of CD14⁺ at the indicated T cells:monocyte ratio (left); proliferation of CD8⁺ is shown (right). FC, fold change by using as the calibrator untreated monocytes; AU, arbitrary units. P<0.001 by paired Student's *t*-test (B,C left panels). *P<0.05, **P<0.01 by paired Student's *t*-test (C right panels, F). *P<0.05 by Mann-Whitney *U*-test (E). For (B) and (C) experiments were repeated twice and performed in triplicates.

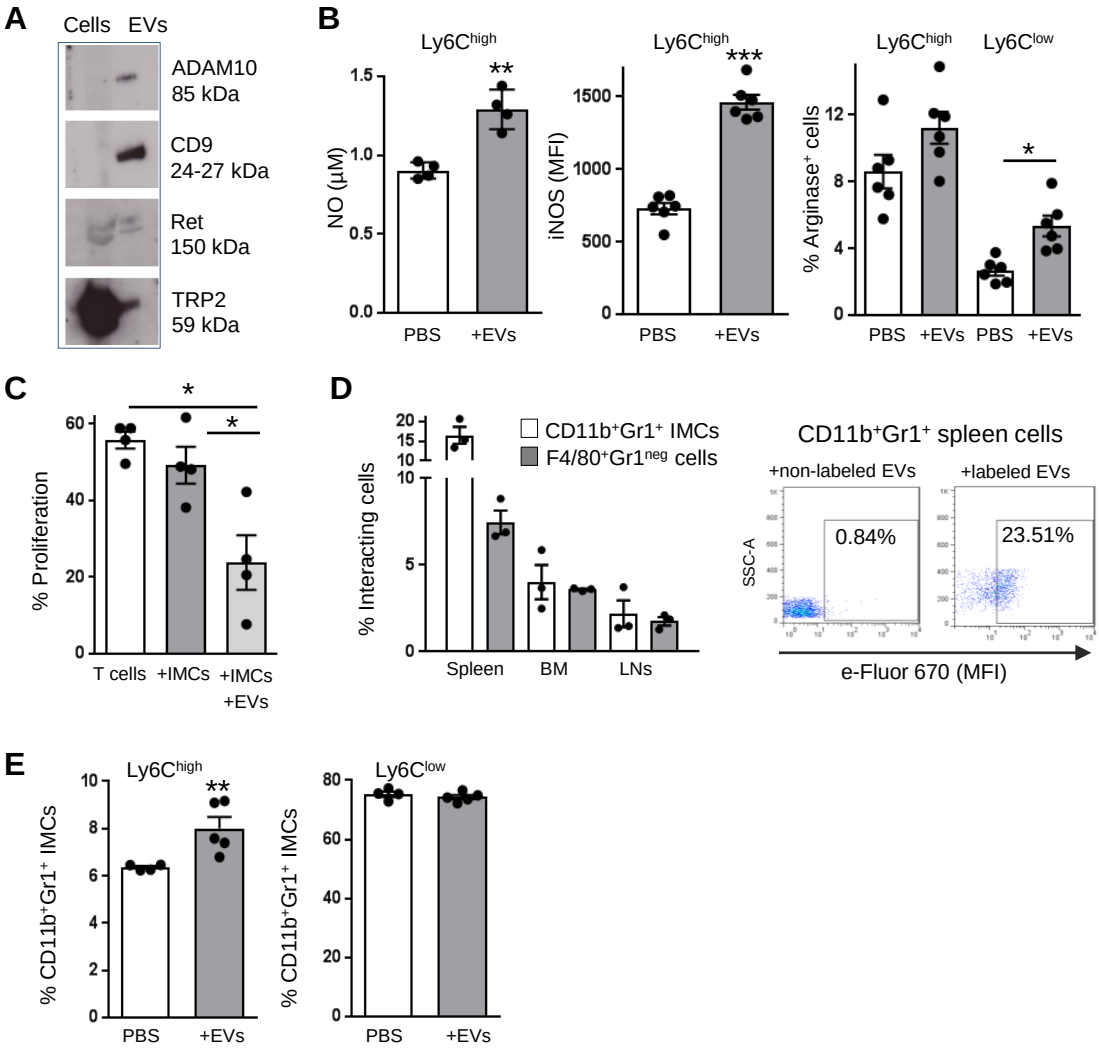

Supplemental Figure 2. Melanoma EV induction of MDSC phenotype in vivo. (**A**) Analysis of *ret* murine melanoma cells and *ret*-derived EVs by Western blot. (**B**) Increased NO production and iNOS expression in BM-derived CD11b⁺Gr1⁺ cells after in vitro incubation with *ret*-EVs (left). Arginase-I expression by monocytic and granulocytic subsets of CD11b⁺Gr1⁺ IMCs from BM after in vitro incubation for 20 h with *ret*-EVs, as measured by flow cytometry (right). (**C**) Proliferative response of T cells cultured with CD11b⁺Gr1⁺ IMCs treated or not with *ret*-EVs. (**D**) Interaction of murine CD11b⁺Gr1⁺ IMCs and F4/80⁺Gr1^{neg} macrophages with *ret*-EVs after i.p. injection (left). In vivo uptake of e-Fluor 670-labeled melanoma *ret*-EVs by CD11b⁺Gr1⁺ spleen cells evaluated by flow cytometry (right). (**E**) Increased frequency of the Ly6C^{high} monocytic MDSC subset compared to Ly6C^{low} cells in BM-CD11b⁺Gr1⁺ cells as evaluated by flow cytometry after *ret*-EVs i.p. injection. MFI, mean fluorescence intensity. Data are presented as mean ± SEM. *P<0.05, **P<0.01, ***P<0.001 by paired and unpaired (E) Student's *t*-test. At least three independent experiments were performed with n=3-6 animals/group.

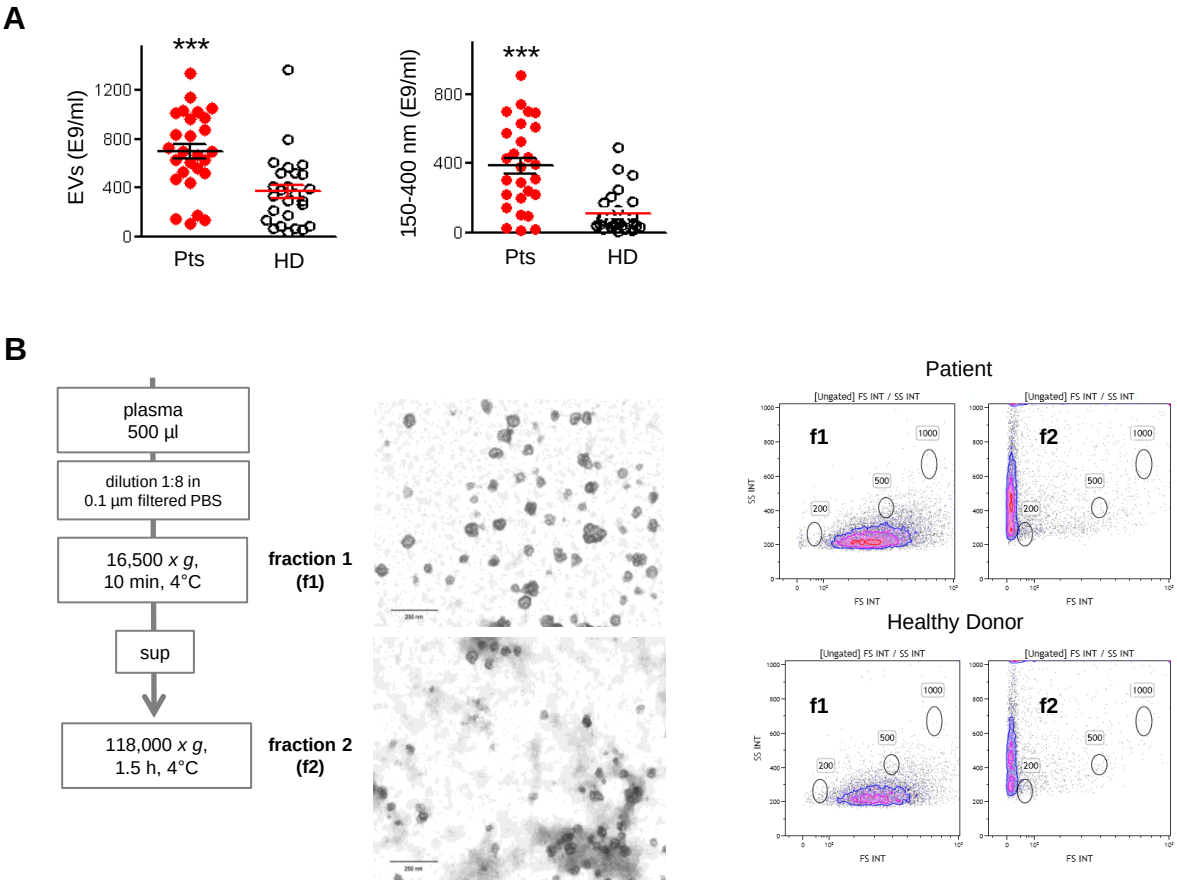

Supplemental Figure 3. Isolation of plasma EVs. (**A**) NTA evaluation of EV number and size in plasma samples of patients and HD (n=27/group). (**B**) Plasma samples were processed to obtain f1 and f2 and evaluated by TEM (left). Fractions, isolated from plasma of a healthy donor and a melanoma patient, were analyzed by flow cytometry using a Gallios flow cytometer calibrated with 200 nm, 500 nm and 1000 nm beads. Representative dot plots are shown (right). ***P < 0.001 by unpaired Student's *t*-test.

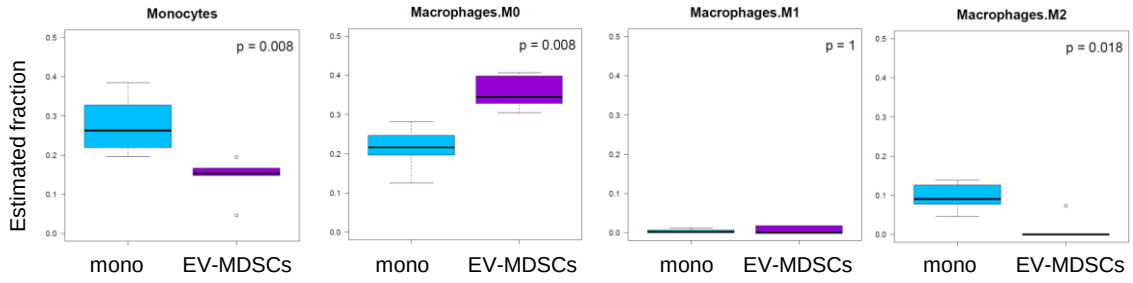

Supplemental Figure 4. CIBERSORT analysis of EV-MDSCs. CIBERSORT analysis of GEP data obtained from monocytes vs EV-MDSCs. EV-MDSCs associate with a M0 profile.

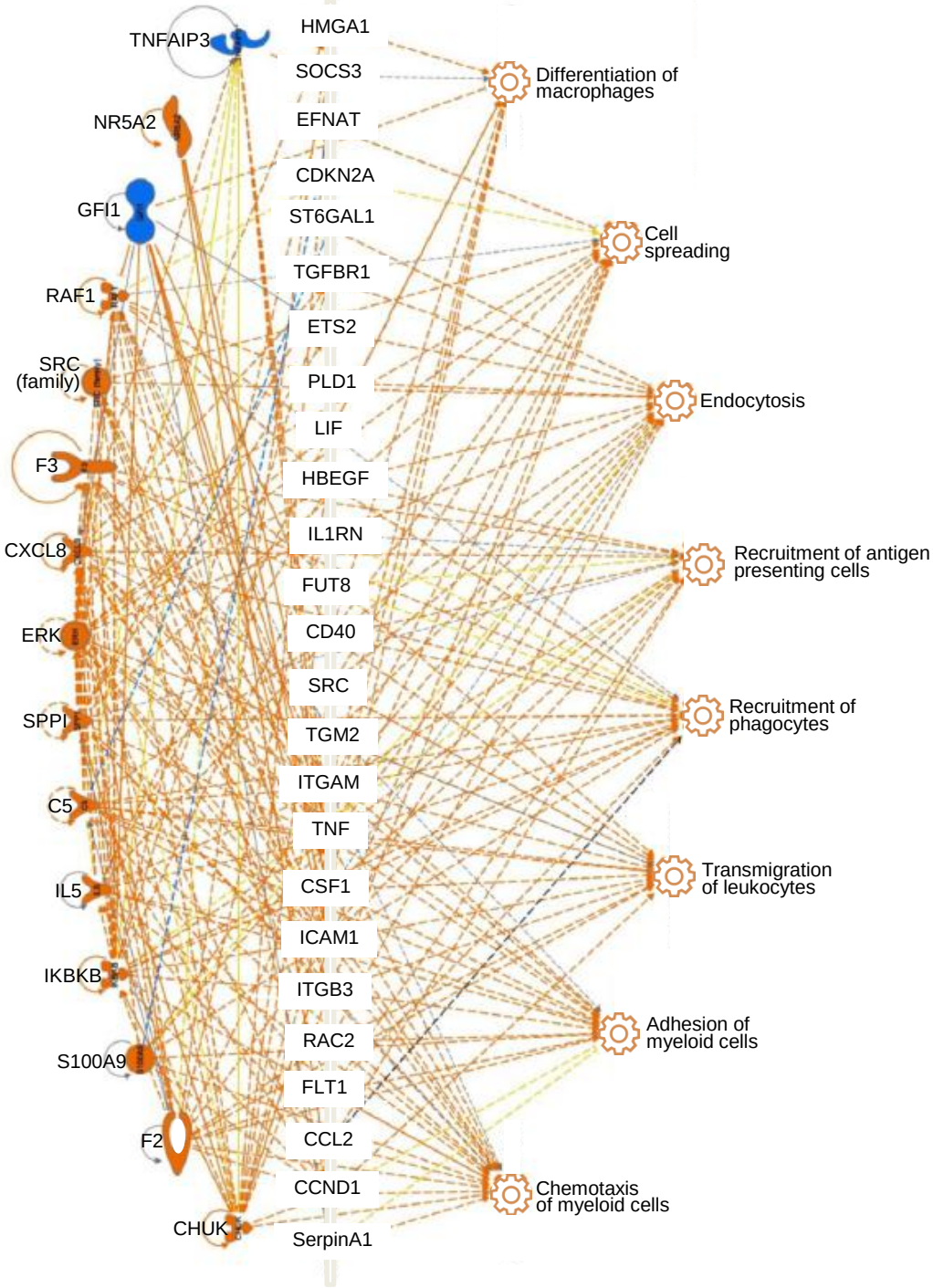

Supplemental Figure 5. Analysis of gene and miR expression profiles of EV-MDSCs. Ingenuity Pathway Analysis (IPA) of EV-MDSCs regulated genes targeted by miRs revealed a main network controlling functions of myeloid cells, including chemotaxis, adhesion, differentiation, recruitment of phagocytes, macrophages and antigen presenting cells, connecting 25 regulated genes to 15 upstream regulators.

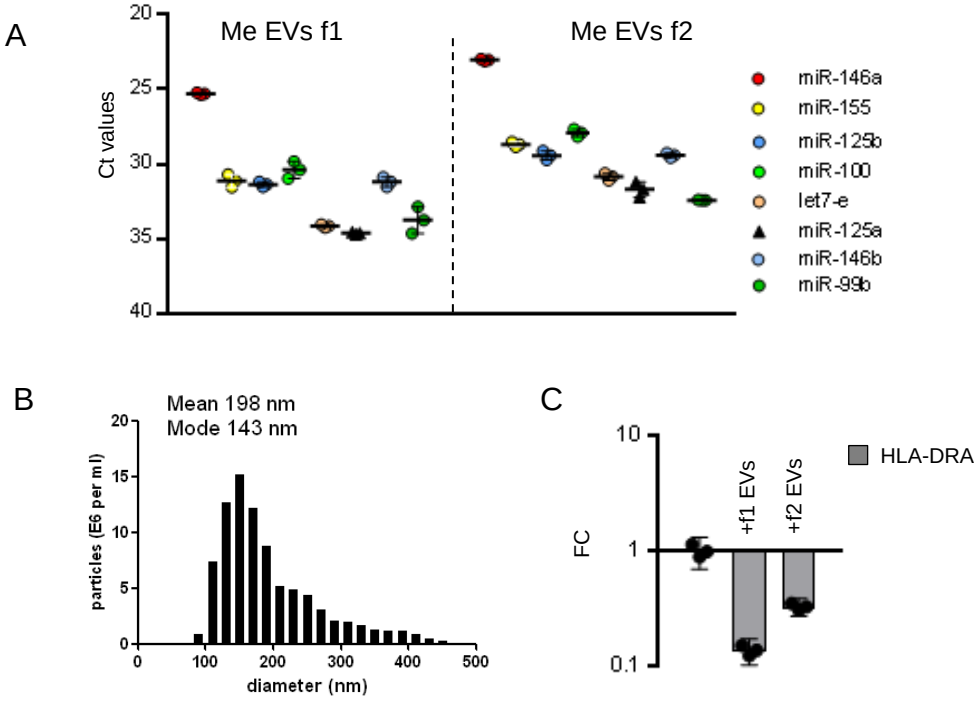

Supplemental Figure 6. Melanoma EVs fractions. (**A**) Expression of MDSC-miRs in f1 and f2 melanoma EV fractions. (**B**) Particle concentration and distribution of melanoma EVs in cell-depleted CM of INT12 melanoma cells measured by NTA. Representative data of 5 measurements is shown. (**C**) MDSC conversion of monocytes by f1 and f2 melanoma EVs. FC, fold change by using as calibrator untreated monocytes. P<0.05 by paired *t* test (C). Experiments in A and C were performed in triplicates and repeated twice.

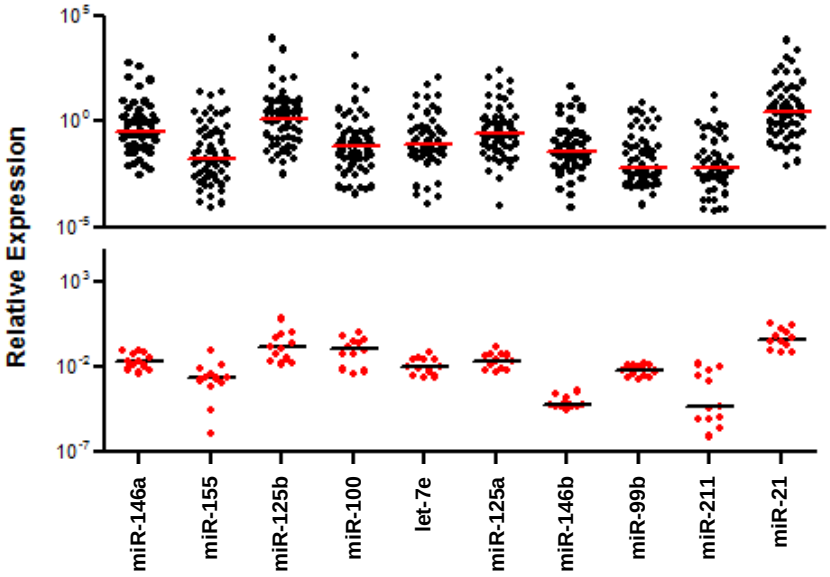

Supplemental Figure 7. MDSC-miR expression in melanoma. miR expression levels in metastatic specimens (upper panel, black dots) and in melanoma cell lines (lower panel, red dots). Melanoma specimens, n=58; melanoma cell lines, n=12. miR-21 and miR-211 were included as unrelated positive control miRs. Relative expression levels and median are shown, as resulting from $2^{-\Delta Ct}$ (log10) values.

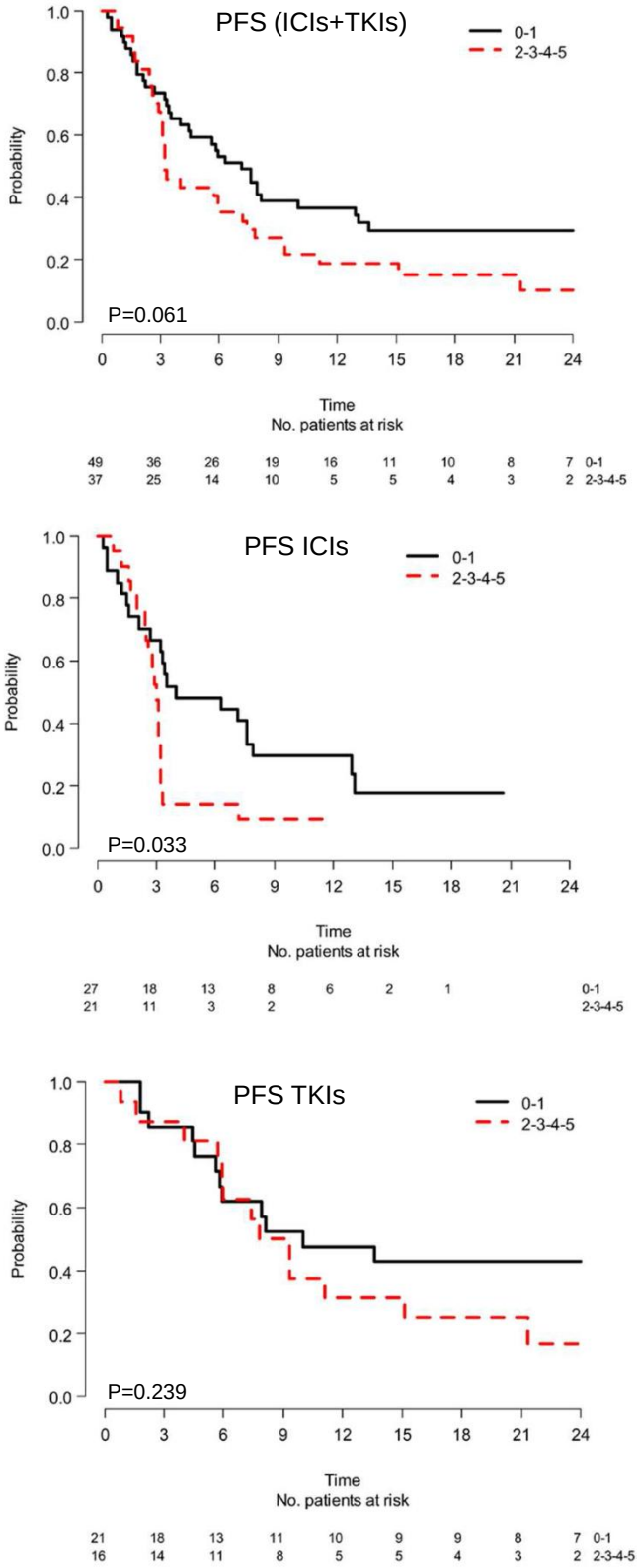

Supplemental Figure 8. MDSC-miR plasma levels associate to resistance to immunotherapy. Progression free survival (PFS) of metastatic melanoma patients based on the expression levels of MDSC-miRs in plasma samples obtained at baseline of therapy, assessed by multivariable index score approach and AIM, in the global population (n=86; for one patient of the global population PFS was missing; upper panel) and in the subsets of patients receiving immunotherapy (ICIs, n=48) or targeted therapy (TKIs, n=37). One patient was excluded from the latter analysis because receiving chemotherapy. Patients with low scores (0-1; showing no or only one increased miR) had a significantly better PFS with respect to patients with high scores (2-5; having 2-5 increased miRs) only if receiving ICIs. Kaplan-Meier survival curves with Log-rank p-values are shown.